

**( $P, T$ ) phase boundary in Li-intercalated graphite: Theory and experiment**D. P. DiVincenzo,\* C. D. Fuerst,<sup>†</sup> and J. E. Fischer<sup>‡</sup>*Laboratory for Research on the Structure of Matter, University of Pennsylvania,  
Philadelphia, Pennsylvania 19104*

(Received 10 November 1983)

A simultaneous stage change and in-plane order-disorder transition is observed in dilute stage-2 Li-intercalated graphite either at low temperature or high pressure. Classical thermodynamics correctly predicts the observed slope of the equilibrium line in the ( $P, T$ ) plane, justifying the Bragg-Williams approximation for the configurational entropy.

Despite the recent success<sup>1</sup> of the simplest microscopic staging model<sup>2</sup> for graphite intercalation compounds (GIC's), it is not clear that it is adequate for describing phase transitions which occur at high pressure. For example, we have found<sup>3</sup> that  $\text{KC}_8$  transforms to a fractional stage- $\frac{3}{2}$  compound at 15 kbar and 300 K. In this as well as in other pressure phase transitions (e.g.,  $\text{KC}_{24}$ ,  $\text{RbC}_{48}$ ) (Ref. 4) a change of stage is found to be intimately associated with a change of in-plane intercalant density. The applicability of the mean-field theory to this phenomenon has not been previously investigated.

In this Rapid Communication we report the experimental observation of a pair of phase transitions which shed new light on the problem of extending the mean-field description of intercalation compounds to include pressure-induced transitions. We find that dilute stage-2 Li-intercalated graphite undergoes simultaneous changes in stage and in-plane density at high pressure, similar to  $\text{KC}_8$ ,  $\text{KC}_{24}$ , and  $\text{RbC}_{48}$ . In addition, this compound also exhibits the *same* phase transformation at *zero*  $P$  and *low*  $T$ . This suggests an intimate connection between the  $P=0$  phase diagram (whose features can be accurately reproduced by a mean-field model in Li-intercalated graphite<sup>5</sup>) and  $P > 0$  phase transformations. We have constructed a simple thermodynamic argument within the mean-field theory which explains the relationship between  $T$  and  $P$  phase transitions in a physically appealing way. This theory gives a quantitatively accurate prediction of the observed stage-2 Li-intercalated graphite phase boundary, and suggests that the mean-field model should be appropriate for unifying the previously unrelated  $T$  and  $P$  experiments on an entire class of intercalation compounds.

Stage-2 Li-intercalated graphite is unique among GIC's in that it occurs in two forms, dense and dilute.<sup>6</sup> The dense  $\text{LiC}_{12}$  is three-dimensionally (3D) ordered and exhibits the same  $\sqrt{3} \times \sqrt{3}$  in-plane superlattice as stage-1  $\text{LiC}_6$ . The dilute compound is disordered at 300 K;<sup>6</sup> its stoichiometry was estimated as  $\text{LiC}_{18 \pm 1}$  from x-ray photoemission spectroscopy (XPS) core-level intensities.<sup>7</sup> We observe structural phase transitions at low  $T$  or high  $P$  in the dilute but not the dense variety, consistent with the combined staging and in-plane ordering transition originally discovered in  $\text{KC}_{24}$  at 7 kbar.<sup>4</sup> Figure 1 shows the relative  $c$ -axis resistivity versus  $T$  for heating and cooling of the dilute sample at  $P=1$  atm. Cooling from the high- $T$  phase initially gives a weakly nonmetallic behavior terminated by an abrupt threefold increase at 250 K. Below this temperature  $\rho_c$  is weakly metallic and can be cycled repeatedly with no hysteresis. Warm-

ing above 250 K, we find the first evidence of a corresponding  $\rho_c$  decreased at 272 K; waiting for equilibrium at 287 K (which requires 3 days) still leaves 80% of the  $\rho_c$  increase to be recovered at yet higher temperatures. Leaving a sample at 296 K for an additional 3 days returns  $\rho_c$  to its initial value; thus the upper critical temperature is between 287 and 296 K.

The large abrupt  $\rho_c$  increase at low  $T$  is suggestive of a staging transition, by analogy to our previous studies of K-intercalated graphite at high pressure.<sup>3,8</sup> The 300-K (00 $l$ ) x-ray diffractogram shows single phase stage 2 with no detectable staging disorder.<sup>3</sup> The inset to Fig. 1 shows the 240-K equilibrium diffractogram recorded 200 h after cooling from room temperature. New reflections from a stage-3 sequence emerge at the expense of the strength of the stage-2 (00 $l$ )'s. Once again we find no evidence for staging disorder in either of the low- $T$  phases. Whereas the Li in the 300-K stage-2 phase is disordered, both constituents of the low- $T$  phase are fully 3D ordered. Interlayer scans along  $(\sqrt{3} \times \sqrt{3})$  and carbon rows show that the stage-2 frac-

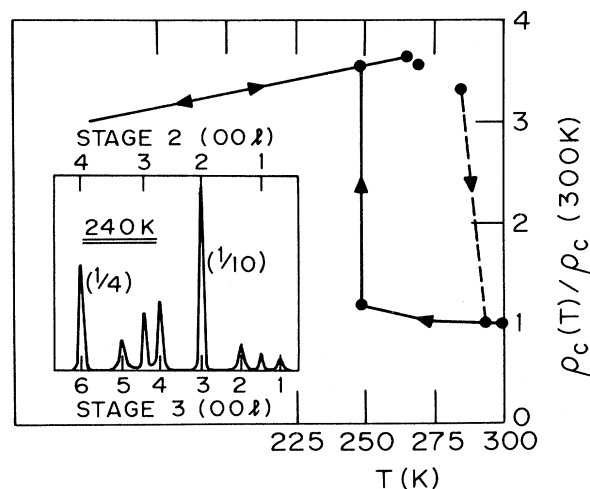


FIG. 1. Temperature-dependent  $c$ -axis resistivity (normalized to 300 K) for dilute stage-2 Li-intercalated graphite. Solid lines connect closely spaced equilibrium data points, a few of which are emphasized to bring out the hysteresis. The dashed line is a guide to the eye. The transition occurs discontinuously at  $248 \pm 1$  K upon cooling; the upper  $T_c$  is close to ambient and was not studied in detail. Inset: x-ray diffractogram at 240 K, showing emergence of stage 3 as one component of the low- $T$  phase.

tion which persists at low  $T$  is  $\text{LiC}_{12}$  ( $AA\alpha AA\alpha \dots$ ) and the new stage-3 phase is  $\text{LiC}_{18}$  with most probable stacking sequence  $ABA\alpha ABA\alpha \dots$ .<sup>9</sup> With these identifications of the low- $T$  phase, we can estimate the molar fractions of stage 2 and stage 3 as 0.31 and 0.69, respectively. Further, since the transition is completely reversible, we can infer that the 300-K Li density corresponds to  $\text{LiC}_{16}$  rather than  $\text{LiC}_{18}$ .

Figure 2 shows the  $T=300$  K, high-pressure complement of Fig. 1. Initially,  $\rho_c$  of dilute stage-2 Li-intercalated graphite is constant up to 1.5 kbar. We then find a slow  $\rho_c$  increase which is evidently a precursor to a transition at 2.9 kbar at which  $\rho_c$  increases by a factor of 2. In the high- $P$  phase  $\rho_c$  is stable and continuous in the range 0.5–4.5 kbar, exhibiting a small negative  $d\rho_c/dP$  consistent with deformation effects. Reversal of the transition requires removing the sample from the cell, since the minimum pressure to maintain the seal exceeds the lower critical pressure. At 1 atm, three days are required for  $\rho_c$  to relax to its initial value. This permitted us to remove the sample, remount it for x rays, and record a (00 $l$ ) diffractogram within 1 h of beginning the descent from the high- $P$  phase; this is shown as the inset to Fig. 2. Again we see a mixture of stages 2 and 3 with approximately the same intensity ratios as in the low- $T$  experiment. The similarity of Figs. 1 and 2 strongly suggest that the high- $P$  and low- $T$  phases are entirely equivalent.

Pressure can be very simply included in a mean-field theory, as we now show. Structural degrees of freedom are included<sup>2</sup> in parameters  $\{\sigma_j\}$  which represent the average concentration in the  $j$ th intercalant layer,  $\sigma_j=1$  representing a saturated, fully ordered layer and  $\sigma_j=0$  an empty layer. The zero-pressure free energy at temperature  $T$  is<sup>2</sup>

$$F_0(T) = E_0(\{\sigma_j\}) - \mu \sum_j \sigma_j + kT \sum_j [(1 - \sigma_j) \ln(1 - \sigma_j) + \sigma_j \ln \sigma_j] . \quad (1)$$

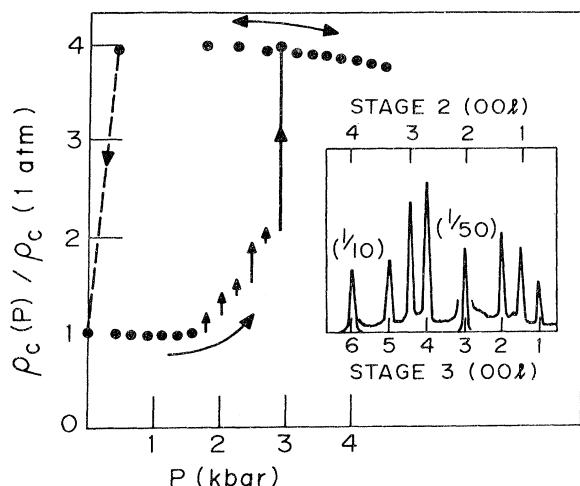


FIG. 2. High-pressure (300 K) analog of Fig. 1. The short arrows represent slow kinetic effects observed after each  $P$  increment; at 2.9 kbar,  $d\rho_c/dt$  increases by at least a factor of 10 and the end point is reached in 16 h. The 2.9-kbar discontinuity is analogous to the 250-K, 1-atm anomaly in Fig. 1 as evidenced by the nearly identical diffractograms in high- $P$  (inset) and low- $T$  (Fig. 1 inset) mixed phases.

Here the last term represents the Bragg-Williams entropy  $S$  of the system,  $\mu$  is the external chemical potential, and  $E_0(\{\sigma_j\})$  is the energy of the system at  $T=0$ . To include finite pressure in this model, we propose a simple modification to Eq. (1):

$$F(P, T) = F_0(T) + P \sum_j \Omega(\sigma_j) , \quad (2)$$

where  $\Omega(\sigma_j)$  is the volume per intercalant site (i.e., per six C atoms) of layer  $j$ . A first approximation for  $\Omega(\sigma_j)$  in graphite intercalation compounds which is known to be reasonable<sup>1,10</sup> is  $\Omega(\sigma_j) = \Omega_0$  if  $\sigma_j=0$ , or  $\Omega(\sigma_j) = \Omega_0 + \Delta\Omega$  if  $\sigma_j > 0$ ; in Li-intercalated graphite,  $\Delta\Omega = 5.5 \text{ \AA}^3$ . The essential assumptions are that pressure enters only through the  $PV$  term and does not affect the fundamental interactions among the constituents as represented by  $E_0$ , and that the entropy is  $T$  and  $P$  independent, having the mean-field form. It is also assumed that the in-plane energy term  $E_0(\{\sigma_j\})$  possesses two local minima, one for in-plane coverage  $\sigma_j^A = 1$  per  $\sqrt{3} \times \sqrt{3}$  lattice gas site, the other near  $\sigma_j^B \cong 0.75$  per site. This structure is consistent with the experimental observation of only two discrete in-plane concentrations and is likely to originate from the combined effects of the host "corrugation" potential and the intrinsic alkali-alkali interaction.<sup>11</sup> In the analysis below we assume that the system chooses between the discrete layer concentrations  $\sigma_j^A$  and  $\sigma_j^B$ . Despite this imposed discreteness, it is still appropriate to use the mean-field entropy. In a dense  $\sqrt{3} \times \sqrt{3}$  ordered layer,  $S=0$  is correctly predicted by Eq. (1). A dilute layer, while it also has a low total energy  $E_0$ , has no anomaly in its entropy since it is experimentally disordered. Thus no more error is made by evaluating the entropy with reference to the  $\sqrt{3} \times \sqrt{3}$  sites than in the original model.<sup>2</sup> (Note also that since  $S$  is the logarithm of the configurational degeneracy, only its order of magnitude need be estimated correctly.) On the other hand, if both the dense and dilute phases were ordered (as in  $\text{KC}_8$  at high pressure<sup>3</sup>), the present analysis would require modification.

We now use the free-energy model of Eq. (2) to study the experiments described above. The actual position of the phase equilibrium line in the  $(P, T)$  plane, given by the condition  $F_i(P, T) = F_f(P, T)$  ( $i$  = initial, dilute;  $f$  = final, dense), is strongly dependent on all the basic energetic parameters contained in  $E_0$ . These parameters are rather difficult to estimate.<sup>2</sup> By contrast, the slope of the phase equilibrium line as given by the Clausius-Clapeyron equation<sup>12</sup>  $dP/dT = (S_f - S_i) / (\Omega_f - \Omega_i)$  is easy to compute in the mean-field model. In the initial dilute stage-2 phase ( $T_i = 296$  K,  $P = 0$ ), the layer sequence is  $\{\sigma^B, 0, \sigma^B, 0, \dots\}$ , the entropy per site is

$$S_i = -\frac{1}{2}k[\sigma^B \ln \sigma^B + (1 - \sigma^B) \ln(1 - \sigma^B)] ,$$

and the volume per site is  $\Omega_i = \frac{1}{2}(2\Omega_0 + \Delta\Omega)$ . The final state, either at low  $T$  (240 K,  $P = 0$ ) or high  $P$  (295 K, 3 kbar) consists of a mixed phase with proportion  $x$  of ordered dense stage 2  $\{\sigma^A, 0, \sigma^A, 0, \dots\}$  and proportion  $(1-x)$  of ordered dense stage 3  $\{\sigma^A, 0, 0, \sigma^A, 0, 0, \dots\}$ . The final-state free energy is obtained by a Maxwell construction:  $F_f = xF_2 + (1-x)F_3$ . The final entropy  $S_f$  is zero, and

$$\Omega_f = x(2\Omega_0 + \Delta\Omega)/2 + (1-x)(3\Omega_0 + \Delta\Omega)/3 .$$

Reversibility implies constant Li concentration whence  $x = 3\sigma^B/\sigma^A - 2$ . The final result,  $dP/dT = 0.057$  kbar/K, is given by the dashed line in Fig. 3. Since the transition is strongly first order and hysteretic (see Figs. 1 and 2), the actual phase boundary is not directly accessible. The edges of this loop are known at four places in the (P,T) plane, as indicated by solid dots and error bars in Fig. 3. The solid lines are drawn with the theoretical slope and they pass through the experimental points perfectly. It is thus reasonable to infer that our model provides an accurate description of the true phase boundary; while further rigorous justification is needed, it appears that our assumptions are justified in the Li-graphite system.

The above model provides a simple explanation of the fundamental relationship between low-T and high-P phase transitions. The key to linking the two lies in the fact that in the ambient state the intercalant layers are not maximally dense. Increased density affects the free energy in two ways: the intercalant takes on an ordered commensurate in-plane superlattice, reducing  $S$  to zero; and the overall volume decreases as some or all of the sites go from  $\sigma^B$  to  $\sigma^A$ . Low  $T$  favors low  $S$  while high  $P$  favors low  $V$ , thus either low  $T$  or high  $P$  can induce the transition. This picture supports the point of view that the staging transition is driven by the change in in-plane density rather than the converse.

It is now easy to see why this phase transformation is manifested most dramatically by the Li-graphite system. The slope of the phase equilibrium line is inversely proportional to  $\Delta\Omega$ , the change of volume upon intercalation.  $\Delta\Omega$  is smaller in Li-intercalated graphite than in any other GIC and therefore  $dP/dT$  is greatest in this system. The transition<sup>4</sup>  $\text{KC}_{2 \times 12} \rightarrow \text{KC}_{3 \times 8}$  at 7 kbar involves a  $\Delta\Omega$  ten times larger than in the present case; we predict that this transition will not extrapolate to positive  $T$  at  $P=0$ , although the critical pressure would decrease to 5 kbar at

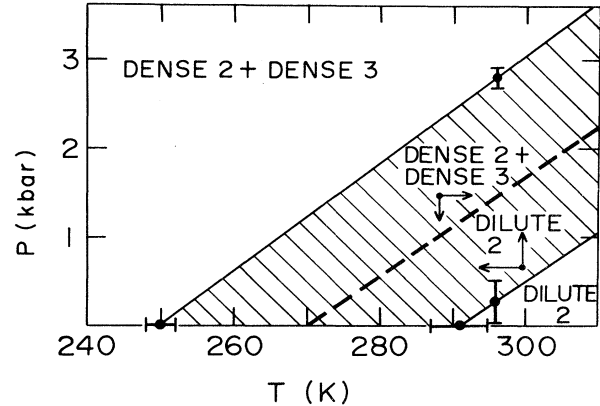


FIG. 3. (P,T) phase diagram for  $\text{LiC}_{16}$ . Dots and error bars are the extremities of the  $\rho_c(T,P)$  hysteresis loops in Figs. 1 and 2. The dashed line shows the predicted slope of the equilibrium phase line. Solid lines drawn parallel to the dashed line can be displaced so as to lie on the data points. The stable phases are dilute 2 (lower right) and mixed dense 2+3 (upper left); in the hatched region either phase is stable depending on past history.

$T=0$ . Still, the Clausius-Claperyon relationship should be of great value in guiding future experiments in the (P,T) plane, and in further establishing the connection between theory and experiment. An excellent candidate would be  $\text{Li}_x\text{TiS}_2$  which is stage 1 for all  $x$  at 300 K and 1 atm.

We thank H. Mertwoy and J. W. Milliken for sample preparation and J. B. Hastings for assistance in performing the x-ray experiments. This work is supported by the National Science Foundation—Materials Research Laboratories Program Grant No. DMR-82-16718.

\*Also at Physics Department, University of Pennsylvania, Philadelphia, PA 19104.

†Also at Physics Department, University of Pennsylvania, Philadelphia, PA 19104. Current address: General Motors Research Laboratory, Warren, MI 48090.

‡Also at Department of Materials Science and Engineering, University of Pennsylvania, Philadelphia, PA 19104.

<sup>1</sup>K. C. Woo, H. Mertwoy, J. E. Fischer, W. A. Kamitakahara, and D. S. Robinson, *Phys. Rev. B* **27**, 7831 (1983); see also R. Clarke, N. Caswell, and S. A. Solin, *Phys. Rev. Lett.* **42**, 61 (1979).

<sup>2</sup>S. A. Safran, *Phys. Rev. Lett.* **44**, 937 (1980); *Synth. Met.* **2**, 1 (1980); S. E. Millman and G. Kirczenow, *Phys. Rev. B* **26**, 2310 (1982); S. E. Millman, G. Kirczenow, and D. Solenberger, *J. Phys. C* **15**, L1269 (1982).

<sup>3</sup>C. D. Fuerst, J. E. Fischer, J. D. Axe, J. B. Hastings, and D. B. McWhan, *Phys. Rev. Lett.* **50**, 357 (1983).

<sup>4</sup>R. Clarke, N. Wada, and S. A. Solin, *Phys. Rev. Lett.* **44**, 1616 (1980); N. Wada, *Phys. Rev. B* **24**, 1065 (1981).

<sup>5</sup>D. P. DiVincenzo (unpublished).

<sup>6</sup>K. C. Woo, W. A. Kamitakahara, D. P. DiVincenzo, D. G. Robinson, H. Mertwoy, J. W. Milliken, and J. E. Fischer, *Phys. Rev. Lett.* **50**, 182 (1983).

<sup>7</sup>S. B. DiCenzo, S. Basu, and G. K. Wertheim, *Synth. Met.* **3**, 139 (1981).

<sup>8</sup>C. D. Fuerst, D. Moses, and J. E. Fischer, *Phys. Rev. B* **24**, 7471 (1981).

<sup>9</sup>The sequence  $AAA\alpha$ , although unlikely on physical grounds, cannot be ruled out by the diffraction data.

<sup>10</sup>P. Hawrylak and K. R. Subbaswamy, *Phys. Rev. B* **28**, 4851 (1983).

<sup>11</sup>D. P. DiVincenzo and E. J. Mele, in *Intercalated Graphite*, edited by M. S. Dresselhaus, G. Dresselhaus, J. E. Fischer, and M. J. Moran (North-Holland, New York, 1983), p. 123.

<sup>12</sup>F. Reif, *Fundamentals of Statistical and Thermal Physics* (McGraw-Hill, New York, 1965), p. 304.